

Molecular structure of [Tl(tpp)(O₂CCF₃)] and ¹⁹F dynamic nuclear magnetic resonance of it and [Tl(tmpp)(O₂CCF₃)] [tpp = 5,10,15,20-tetraphenylporphyrinate, tmpp = 5,10,15,20-tetra(4-methoxyphenyl)-porphyrinate]

Lung-Fang Chou and Jyh-Horung Chen *

Department of Chemistry, National Chung-Hsing University, Taichung 40227, Taiwan, Republic of China

The crystal structure of (*meso*-5,10,15,20-tetraphenylporphyrinato)(trifluoroacetato)thallium(III), [Tl(tpp)(O₂CCF₃)], was determined. The co-ordination sphere of the Tl³⁺ ion is an approximate square-based pyramid in which the apical site is occupied by an asymmetric bidentate O₂CCF₃⁻ group. The average Tl–N bond distance is 2.200(5) Å and the Tl atom is displaced 0.741 Å from the porphyrin plane. The Tl–O(1) and Tl–O(2) distances are 2.309(7) and 2.64(1) Å, respectively. The extent of dissociation of [5,10,15,20-tetra(4-methoxyphenyl)porphyrinato](trifluoroacetato)thallium(III), [Tl(tmpp)(O₂CCF₃)], in CD₂Cl₂ was ≈4%. The free energy of activation at the coalescence temperature *T*_c was for the intermolecular trifluoroacetate exchange between ≈96 of [Tl(tmpp)(O₂CCF₃)] and ≈4% of CF₃CO₂H in CD₂Cl₂ solvent has been found to be Δ*G*₂₃₈[‡] 45.8 kJ mol⁻¹ through ¹⁹F NMR temperature-dependent measurements. However, [Tl(tmpp)(O₂CCF₃)] and its homologue [Tl(tpp)(O₂CCF₃)] do not dissociate in [²H₈]tetrahydrofuran. They undergo intramolecular CF₃CO₂⁻ exchange in this solvent and Δ*G*₂₁₂[‡] (or Δ*G*₂₀₃[‡]) for this process was found to be 44.4 (or 42.0 kJ mol⁻¹) for [Tl(tpp)(O₂CCF₃)] {or [Tl(tmpp)(O₂CCF₃)]} from ¹⁹F dynamic NMR spectroscopy. In the slow-exchange region the CF₃ and carbonyl (CO) carbons of the CF₃CO₂⁻ group in [Tl(tpp)(O₂CCF₃)] are separately located at δ 115.9 [¹J(C–F) = 291, ³J(Tl–¹³C) = 239] and 156.5 [²J(C–F) = 37, ²J(Tl–¹³C) = 128 Hz] at –100 °C.

Although the molecular stereochemistry of (*meso*-5,10,15,20-tetraphenylporphyrinato)(trifluoroacetato)iron(III), [Fe(tpp)(O₂CCF₃)],¹ the synthesis and ¹H NMR spectra of [Tl(tpp)(O₂CCF₃)] and [5,10,15,20-tetra(4-methoxyphenyl)porphyrinato](trifluoroacetato)thallium(III), [Tl(tmpp)(O₂CCF₃)],² the ¹³C NMR spectra of alkyl-substituted aryl thallium bis(trifluoroacetates), [TlR(O₂CCF₃)₂],^{3–6} and the ¹⁹F NMR spectra of [Tl(C₆H₄F-*p*)(O₂CCF₃)₂] and [Tl(C₆H₄F-*p*)₂(O₂CCF₃)] have been reported,⁵ these studies disregarded the ¹⁹F NMR spectra of the trifluoroacetate in the complexes. We were interested in the trifluoroacetate exchange in [Tl(tpp)(O₂CCF₃)] and [Tl(tmpp)(O₂CCF₃)]. The molecular structure and dynamic ¹H NMR studies of their acetate homologues [Tl(tpp)(O₂CMe)]^{7,8} and acetate[*meso*-5,10,15,20-tetra(4-pyridyl)porphyrinato]thallium(III), [Tl(tpyp)(O₂CMe)],⁹ have been reported by our group. It turned out that the acetate exchange in [Tl(tpp)(O₂CMe)] in CD₂Cl₂ was intramolecular,^{7,8} whereas that in [Tl(tpyp)(O₂CMe)] in the same solvent was intermolecular.⁹ The driving force for the intermolecular exchange might be hydrogen bonding between [Tl(tpyp)(O₂CMe)] and acetic acid. In the cases of [Tl(tpp)(O₂CCF₃)] and [Tl(tmpp)(O₂CCF₃)], in the presence of CF₃CO₂H, there might be a similar hydrogen bonding between the trifluoroacetate O of these two complexes and carboxy H of CF₃CO₂H. They could undergo intermolecular trifluoroacetate exchange in CD₂Cl₂ or [²H₈]tetrahydrofuran ([²H₈]thf). In the absence of CF₃CO₂H the intramolecular exchange might be the chief exchange mechanism for these two complexes in [²H₈]thf.

In this paper ¹H and ¹³C NMR spectroscopic studies of [Tl(tpp)(O₂CCF₃)] and [Tl(tmpp)(O₂CCF₃)] and an X-ray analysis of [Tl(tpp)(O₂CCF₃)] are reported. The ¹⁹F NMR spectra of [Tl(tmpp)(O₂CCF₃)] in CD₂Cl₂ (or in [²H₈]thf) and [Tl(tpp)(O₂CCF₃)] in [²H₈]thf at low temperature were examined to infer the inter- and intra-molecular apical ligand

exchange and to determine the free energy of activation at the coalescence temperature, Δ*G*_{*T*_c}[‡], for the exchange process.

Experimental

Preparation of the complexes

The complexes were prepared as previously reported.² Crystals of [Tl(tpp)(O₂CCF₃)], were grown by diffusion of diethyl ether vapour into a CH₂Cl₂ solution. Both complexes were dissolved in CDCl₃ (99.8% from Aldrich), in CD₂Cl₂ (99.95% from Aldrich) or in [²H₈]thf (99.5% from Aldrich). The freshly prepared solutions were poured into several 5 mm NMR tubes. The tubes were then flame-sealed for ¹H, ¹³C or ¹⁹F NMR measurement.

NMR spectra

Proton and ¹³C NMR spectra in CDCl₃, CD₂Cl₂ or [²H₈]thf were recorded at 300.00 (400.13 or 600.20) and 75.47 (100.61 or 150.92) MHz, respectively, on a Bruker MSL-300 (AM-400 or DMX-600) spectrometer locked on solvent deuterium, and referenced to the solvent peak. The ¹⁹F NMR spectra were measured in CD₂Cl₂ (or [²H₈]thf) at 282.40, 376.50 or 564.71 MHz, respectively, on a Bruker MSL-300, AM-400 or DMX-600 spectrometer. Proton and ¹³C NMR are relative to CDCl₃, CD₂Cl₂ or [²H₈]thf at δ 7.24, 5.30 or 1.73 and the centre line of CDCl₃, CD₂Cl₂ or [²H₈]thf at δ 77.0, 53.6 or 25.3; ¹⁹F data are externally relative to CFCl₃. The temperature of the spectrometer probe was calibrated by the shift difference of the methanol resonance in the ¹H NMR spectrum.

Crystallography

Crystal data. [Tl(tpp)(O₂CCF₃)]·CH₂Cl₂, C₄₇H₃₀Cl₂F₃N₄O₂Tl, *M* = 1015.0, triclinic, space group *P* $\bar{1}$, *a* = 11.127(2),

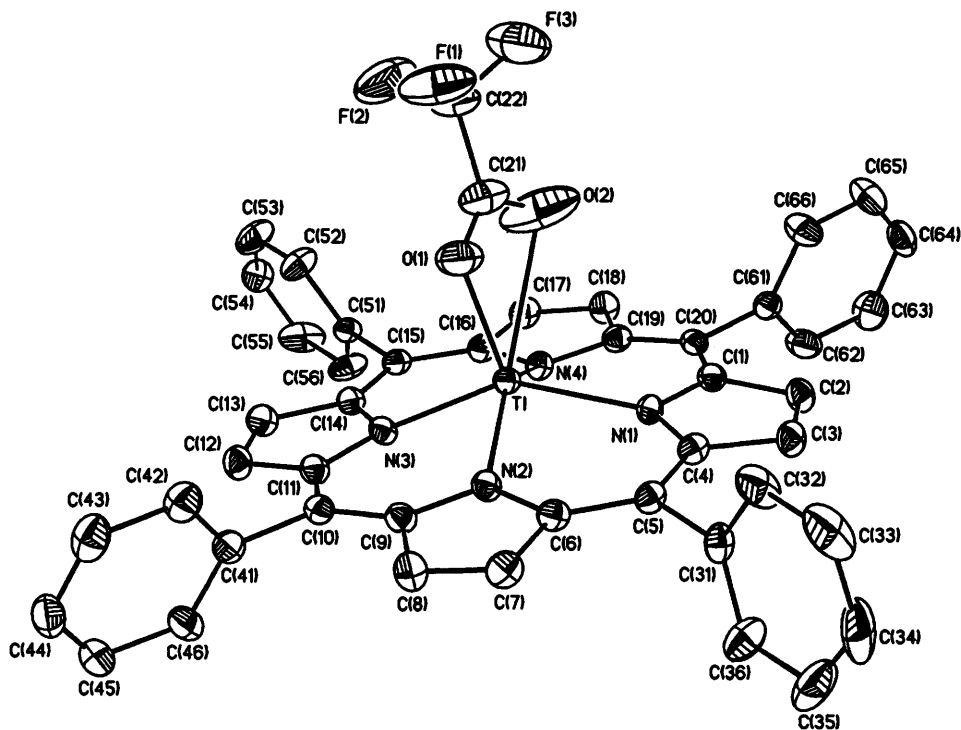


Fig. 1 Molecular configuration and atom labelling scheme for $[\text{Tl}(\text{tp})(\text{O}_2\text{CCF}_3)] \cdot \text{CH}_2\text{Cl}_2$. Hydrogen atoms and solvent C(71)H(71A)H(71B)-Cl(1)Cl(2) are omitted for clarity

$b = 13.297(3)$, $c = 14.706(3)$ Å, $\alpha = 97.51(2)$, $\beta = 94.44(2)$, $\gamma = 103.80(2)^\circ$, $U = 2081.5(8)$ Å³, $Z = 2$, $D_c = 1.619$ g cm⁻³, $F(000) = 996$, $\mu(\text{Mo-K}\alpha) = 40.66$ cm⁻¹, 293 K.

Data collection, structure solution and refinement. X-Ray diffraction data were collected from a crystal of dimensions $0.3 \times 0.5 \times 0.7$ mm on a Siemens R3m/V diffractometer by using crystal-monochromatized Mo-K α radiation ($\lambda = 0.71073$ Å). The θ - 2θ scan technique was used. Of 7682 unique reflections collected up to $2\theta_{\text{max}} = 50^\circ$, 6434 with $F > 4\sigma(F)$ were considered observed and used in the structure analysis. Semiempirical absorption corrections were applied. The structure was solved by direct methods (SHELXTL PLUS).¹⁰ Full-matrix least-squares refinement with anisotropic thermal parameters for all non-hydrogen atoms gave residuals $R = 0.040$ and $R' = 0.054$ {where $R = [\sum |F_o| - |F_c|] / \sum |F_o|$ } and $R' = [\sum w(|F_o| - |F_c|)^2 / \sum w(|F_o|)^2]^{1/2}$. The weighting scheme was $w = [\sigma^2(F) + 0.002F^2]^{-1}$. Hydrogen atom coordinates were calculated using a riding model and included in the refinement (based on F). Selected bond distances and angles are given in Table 1.

Atomic coordinates, thermal parameters, and bond lengths and angles have been deposited at the Cambridge Crystallographic Data Centre (CCDC). See Instructions for Authors, *J. Chem. Soc., Dalton Trans.*, 1996, Issue 1. Any request to the CCDC for this material should quote the full literature citation and the reference number 186/183.

Results and Discussion

Molecular structure of $[\text{Tl}(\text{tp})(\text{O}_2\text{CCF}_3)]$

The skeletal framework of the complex $[\text{Tl}(\text{tp})(\text{O}_2\text{CCF}_3)] \cdot \text{CH}_2\text{Cl}_2$, with $P\bar{1}$ symmetry, is illustrated in Fig. 1. It reveals the six-co-ordination of the thallium atom with four nitrogen atoms of the porphyrinato group and the asymmetric bidentate O_2CCF_3^- ligand. Bond distances (Table 1) are: Tl-O(1) 2.309(7), Tl-O(2) 2.64(1), O(1)-C(21) 1.14(2), O(2)-C(21) 1.21(2), C(21)-C(22) 1.51(2), C(22)-F(1) 1.27(1), C(22)-F(2) 1.28(1), C(22)-F(3) 1.30(2) and mean Tl-N 2.200(5) Å.

Table 1 Selected bond distances (Å) and angles ($^\circ$) for $[\text{Tl}(\text{tp})(\text{O}_2\text{CCF}_3)]$

Tl-O(1)	2.309(7)	C(22)-F(2)	1.28(1)
Tl-O(2)	2.64(1)	C(22)-F(3)	1.30(2)
O(1)-C(21)	1.14(2)	Tl-N(1)	2.184(5)
O(2)-C(21)	1.21(2)	Tl-N(2)	2.212(5)
C(21)-C(22)	1.51(2)	Tl-N(3)	2.197(5)
C(22)-F(1)	1.27(1)	Tl-N(4)	2.206(5)
<hr/>			
Tl-O(1)-C(21)	104.7(8)	O(1)-Tl-N(1)	112.5(2)
Tl-O(2)-C(21)	85.9(9)	O(1)-Tl-N(2)	94.9(2)
O(1)-C(21)-O(2)	120(1)	O(1)-Tl-N(3)	101.8(2)
O(1)-C(21)-C(22)	120(1)	O(1)-Tl-N(4)	121.9(2)
O(2)-C(21)-C(22)	120(1)	O(2)-Tl-N(1)	91.3(3)
C(21)-C(22)-F(1)	114.3(8)	O(2)-Tl-N(2)	137.1(3)
C(21)-C(22)-F(2)	110(1)	O(2)-Tl-N(3)	119.1(3)
C(21)-C(22)-F(3)	111(1)	O(2)-Tl-N(4)	78.6(3)
F(1)-C(22)-F(2)	109(1)	N(1)-Tl-N(2)	84.7(2)
F(1)-C(22)-F(3)	104(1)	N(1)-Tl-N(3)	144.7(2)
F(2)-C(22)-F(3)	107.8(9)	N(1)-Tl-N(4)	84.8(2)
O(1)-Tl-O(2)	47.8(3)	N(2)-Tl-N(3)	84.2(2)
N(3)-Tl-N(4)	84.2(2)	N(2)-Tl-N(4)	143.0(2)

The thallium atom lies 0.683 and 0.741 Å from the four porphyrin nitrogens and the 24-atom porphyrin plane (C_{20}N_4), respectively. The dihedral angles between the mean planes of the skeleton (C_{20}N_4) and the planes of the phenyl groups are 82.4 [C(34)], 70.2 [C(44)], 73.8 [C(54)] and 76.3° [C(64)].

The radius of the central 'hole' ($C_i \cdots N$, distance from the geometrical centre of the mean plane of the 24-atom core to the porphyrinato-core N atoms) in $[\text{Tl}(\text{tp})(\text{O}_2\text{CCF}_3)]$ is 2.092 Å which is larger than 2.01 Å suggested by Collins and Hoard.¹¹ The thallium(III) is bonded in a highly expanded porphyrinato core (C_{20}N_4) and the porphyrin (C_{20}N_4 and Tl) can be regarded as dome shaped. The net doming is ≈ 0.06 Å ($= 0.741 - 0.683$). Fig. 2 shows the displacement (in Å) of each atom of the porphyrin (C_{20}N_4 and Tl) from the porphyrin mean plane (C_{20}N_4). The structure of $[\text{Tl}(\text{tp})(\text{O}_2\text{CCF}_3)]$ is quite different from that of $[\text{Fe}(\text{tp})(\text{O}_2\text{CCF}_3)]$. The core of the

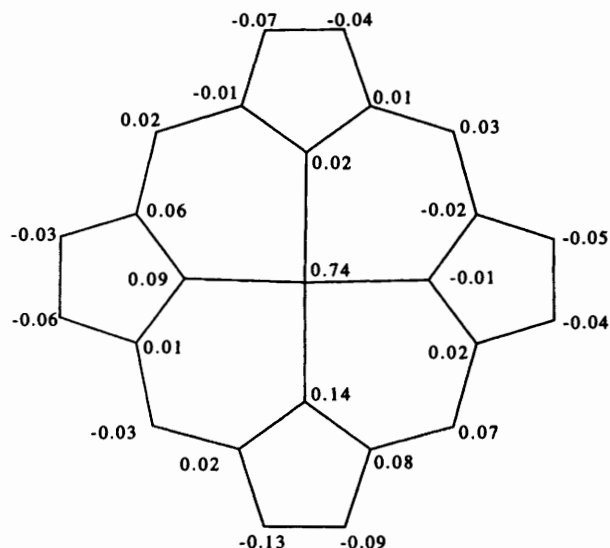
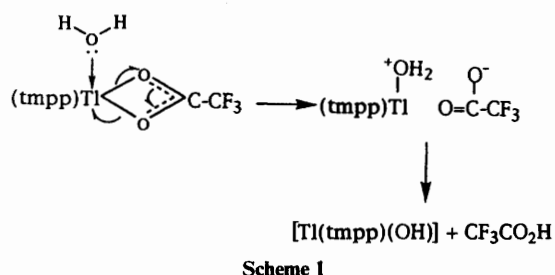


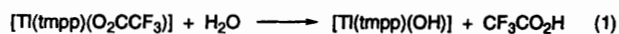
Fig. 2 Diagram of the porphyrin core ($C_{20}N_4$ and Tl) of $[Tl(tpp)(O_2CCF_3)]$ showing the displacement (in Å) of the atoms from the mean plane of the porphyrin ($C_{20}N_4$)



former complex is domed whereas that of the latter complex is a pronounced S_4 ('sad') ruffling.¹ In $[Tl(tpp)(O_2CCF_3)]$ the $O_2CCF_3^-$ is asymmetrically and bidentately co-ordinated to the Tl atom whereas in $[Fe(tpp)(O_2CCF_3)]$ it is unidentate.¹

^{19}F Dynamic NMR investigation

(i) $[Tl(tmpp)(O_2CCF_3)]$ in CD_2Cl_2 . The results of the ^{19}F dynamic NMR studies of $[Tl(tmpp)(O_2CCF_3)]$ in CD_2Cl_2 revealed two stages. The first stage is possibly comprised of hydrolysis of $[Tl(tmpp)(O_2CCF_3)]$ [equation (1)] and



hydrogen bonding between trifluoroacetate O and CF_3CO_2H [equation (2)] where water comes from the CD_2Cl_2 solvent. The production of CF_3CO_2H upon hydrolysis is supported by several reproducible observations of 4% dissociation of $[Tl(tmpp)(O_2CCF_3)]$ in a CD_2Cl_2 -saturated solution at $-70^\circ C$. A hydration constant of $(2.31 \pm 0.06) \times 10^{-4} \text{ mol dm}^{-3}$ is evaluated at this temperature. The second stage involves reversible intermolecular chemical exchange of the $CF_3CO_2^-$ ligand between $[Tl(tmpp)(O_2CCF_3)]$ and CF_3CO_2H . The mechanism of reaction (1) is given in Scheme 1.

When a 0.02 mol dm^{-3} solution of $[Tl(tmpp)(O_2CCF_3)]$ in CD_2Cl_2 (Fig. 3) was cooled the ^{19}F signal of $CF_3CO_2^-$, a single peak at $20^\circ C$ ($\delta -75.35$), first broadened (coalescence temperature $T_c = 238 \text{ K}$) and then split into two sets of peaks (singlet at $\delta -78.07$ and doublet at -75.09) of separation 842 Hz at a frequency of 282.40 MHz. At $-70^\circ C$ the single peak at $\delta -78.07$ corresponds to the trifluoroacetic acid (CF_3CO_2H);

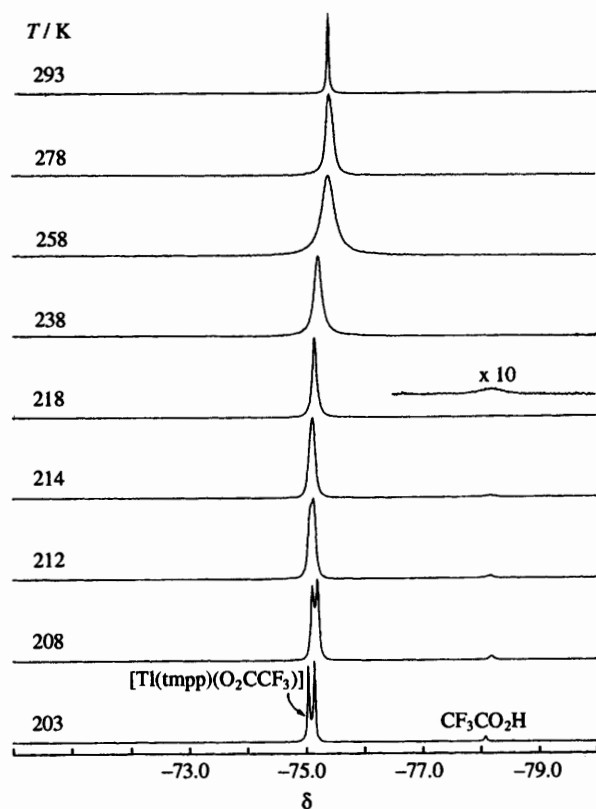
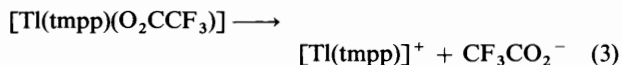


Fig. 3 The 282.40 MHz ^{19}F NMR spectra for the axial $CF_3CO_2^-$ of $[Tl(tmpp)(O_2CCF_3)]$ and for CF_3 of CF_3CO_2H in CD_2Cl_2 at various temperatures

the other doublet peak at $\delta -75.09$, with a separation of 29.8 Hz, is due to a $^4J(Tl-^{19}F)$ coupling of $[Tl(tmpp)(O_2CCF_3)]$. As the exchange of $CF_3CO_2^-$ between $[Tl(tmpp)(O_2CCF_3)]$ and CF_3CO_2H is reversible, this intermolecular process can be treated as a two-site exchange,¹² by taking into account the unequal populations of the two sites, i.e. $\approx 96\%$ of $[Tl(tmpp)(O_2CCF_3)]$ and $\approx 4\%$ of CF_3CO_2H , a comparison of observed and computed spectra yields $\Delta G_{238}^\ddagger = 45.8 \text{ kJ mol}^{-1}$.

For $[Tl(tmpp)(O_2CCF_3)]$ in CD_2Cl_2 the rate-determining step for stage I could either be a bimolecular exchange as in equation (1) or a unimolecular dissociation of the complex [equation (3)] followed by protonation of $O_2CCF_3^-$ [equation (4)]. Since the equilibrium constant for protonation of



$CF_3CO_2^-$ with free water molecules in solution [equation (4)] is $\approx 3.85 \times 10^{-14} \text{ mol dm}^{-3}$ at $25^\circ C$ the forward reaction is a difficult process. If the unimolecular dissociation [equation (3)] and protonation of $O_2CCF_3^-$ [equation (4)] is the chief mechanism, then we cannot explain the observation of CF_3CO_2H originating from the hydrolysis of $[Tl(tmpp)(O_2CCF_3)]$ in CD_2Cl_2 solvent. Obviously the mechanism of unimolecular dissociation is inconsistent with the experimental result.

(ii) $[Tl(tpp)(O_2CCF_3)]$ in $[^2H_6]thf$. When a $3 \times 10^{-2} \text{ mol dm}^{-3}$ solution of $[Tl(tpp)(O_2CCF_3)]$ in CD_2Cl_2 was cooled a spectral frequency of 564.71 MHz, the ^{19}F signal of $CF_3CO_2^-$, a sharp single peak at $20^\circ C$ ($\delta -75.52$, $\Delta v_{\frac{1}{2}} = 2 \text{ Hz}$), became a broad singlet at $-90^\circ C$ with $\Delta v_{\frac{1}{2}} = 66 \text{ Hz}$. It appears that the coalescence temperature (T_c) for the $CF_3CO_2^-$ exchange of $[Tl(tpp)(O_2CCF_3)]$ in CD_2Cl_2 is considerably lower than

–90 °C. Hence, $[\text{Tl}(\text{tpp})(\text{O}_2\text{CCF}_3)]$ was dissolved in $[\text{}^2\text{H}_8]\text{thf}$ for a much lower temperature measurement. When a 0.025 mol dm^{-3} solution of $[\text{Tl}(\text{tpp})(\text{O}_2\text{CCF}_3)]$ in $[\text{}^2\text{H}_8]\text{thf}$ (Fig. 4) was cooled the ^{19}F signal of CF_3CO_2^- , a single peak at 20 °C, first broadened ($T_c = 212 \text{ K}$) then split into two peaks with a separation of 28.6 Hz at –100 °C. As the exchange of CF_3CO_2^- within $[\text{Tl}(\text{tpp})(\text{O}_2\text{CCF}_3)]$ is reversible, the results at 376.50 MHz confirm the separation as a coupling $^4J(\text{Tl}-^{19}\text{F})$ rather than a chemical shift difference. The only fluorine species observed by ^{19}F NMR spectroscopy is $[\text{Tl}(\text{tpp})(\text{O}_2\text{CCF}_3)]$ and the chemical shifts in fast exchange at temperatures above T_c are between two resonances in slow exchange at –100 °C. This is an intramolecular exchange process. A comparison of observed and computed spectra yields $\Delta G_{212}^\ddagger = 44.4 \text{ kJ mol}^{-1}$.¹²

The complex $[\text{Tl}(\text{tpp})(\text{O}_2\text{CCF}_3)]$ does not hydrolyse in $[\text{}^2\text{H}_8]\text{thf}$ or CD_2Cl_2 . Hence, the exchange of CF_3CO_2^- for $[\text{Tl}(\text{tpp})(\text{O}_2\text{CCF}_3)]$ in $[\text{}^2\text{H}_8]\text{thf}$ (or CD_2Cl_2) solvent is intramolecular. If $\approx 0.05 \text{ cm}^3 \text{ CF}_3\text{CO}_2\text{H}$ is intentionally added to the solution of $[\text{Tl}(\text{tpp})(\text{O}_2\text{CCF}_3)]$ in $[\text{}^2\text{H}_8]\text{thf}$ (or CD_2Cl_2) the CF_3CO_2^- exchange switches from intra- to inter-molecular (Fig. 5). At –100 °C the singlet peak with a population of 90% at $\delta -76.70$ corresponds to the added $\text{CF}_3\text{CO}_2\text{H}$ and the other doublet peak with population 10% at $\delta -75.13$ and a separation of 27.2 Hz shown in Fig. 5(b) is due to $[\text{Tl}(\text{tpp})(\text{O}_2\text{CCF}_3)]$. These two peaks arise from slow exchange of CF_3CO_2^- between $[\text{Tl}(\text{tpp})(\text{O}_2\text{CCF}_3)]$ and $\text{CF}_3\text{CO}_2\text{H}$. The slow-exchange limit should be at temperatures below –100 °C. At 20 °C the sharp singlet in Fig. 5(a) is due to fast exchange of CF_3CO_2^- between the former two compounds. The key step for the occurrence of intermolecular CF_3CO_2^- exchange in the complexes $[\text{Tl}(\text{tpp})(\text{O}_2\text{CCF}_3)]$ and $[\text{Tl}(\text{tmpp})(\text{O}_2\text{CCF}_3)]$ is the existence of $\text{CF}_3\text{CO}_2\text{H}$ either externally added or initially present or from hydrolysis.

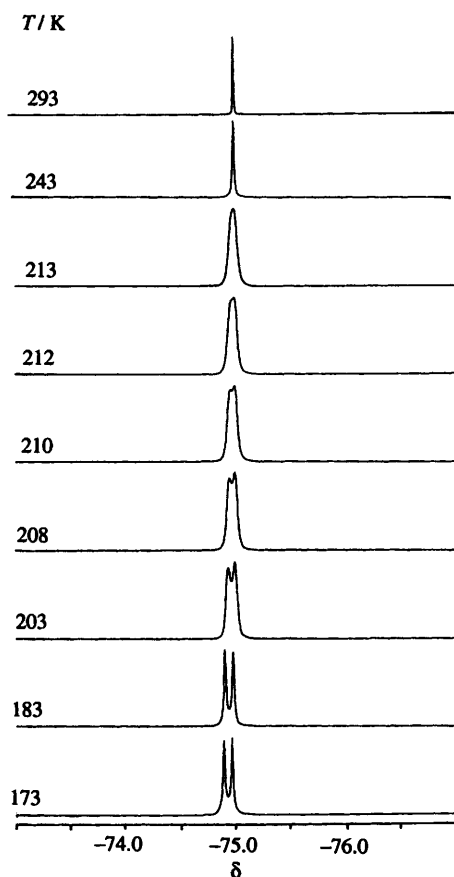
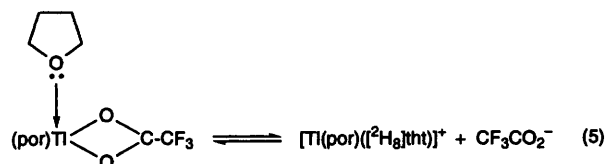


Fig. 4 The 376.50 MHz ^{19}F NMR spectra for $[\text{Tl}(\text{tpp})(\text{O}_2\text{CCF}_3)]$ in $[\text{}^2\text{H}_8]\text{thf}$ at various temperatures

(iii) $[\text{Tl}(\text{tmpp})(\text{O}_2\text{CCF}_3)]$ in $[\text{}^2\text{H}_8]\text{thf}$. The complex $[\text{Tl}(\text{tmpp})(\text{O}_2\text{CCF}_3)]$ does not hydrolyse in $[\text{}^2\text{H}_8]\text{thf}$. It undergoes intramolecular CF_3CO_2^- exchange in this solvent; $\Delta G_{203}^\ddagger = 42.0 \text{ kJ mol}^{-1}$ from ^{19}F dynamic NMR at a frequency of 282.40 MHz {the ^{19}F NMR spectra of $[\text{Tl}(\text{tmpp})(\text{O}_2\text{CCF}_3)]$ in $[\text{}^2\text{H}_8]\text{thf}$ at various temperatures are available from the authors on request}.

In $[\text{}^2\text{H}_8]\text{thf}$ solvent $[\text{Tl}(\text{por})(\text{O}_2\text{CCF}_3)]$ (por = tpp or tmpp) is solvated by a better nucleophile as in equations (5) and (4). As



described above, the forward reaction of equation (4) is a forbidden process, therefore the CF_3CO_2^- formed in (5) recombines with $[\text{Tl}(\text{por})([\text{}^2\text{H}_8]\text{thf})]^+$. This explains why the exchange of CF_3CO_2^- with $[\text{Tl}(\text{por})(\text{O}_2\text{CCF}_3)]$ in $[\text{}^2\text{H}_8]\text{thf}$ is intramolecular. Overall, the mechanism of bimolecular exchange [shown in equations (1) and (5)] explains not only the presence of $\text{CF}_3\text{CO}_2\text{H}$ and $[\text{Tl}(\text{tmpp})(\text{O}_2\text{CCF}_3)]$ in CD_2Cl_2 but also the absence of $\text{CF}_3\text{CO}_2\text{H}$ in solutions of $[\text{Tl}(\text{por})(\text{O}_2\text{CCF}_3)]$ in $[\text{}^2\text{H}_8]\text{thf}$.

^{13}C and ^1H NMR spectra

The ^{13}C NMR data for $[\text{Tl}(\text{tmpp})(\text{O}_2\text{CCF}_3)]$ and $[\text{Tl}(\text{tpp})(\text{O}_2\text{CCF}_3)]$ in CD_2Cl_2 , CDCl_3 or $[\text{}^2\text{H}_8]\text{thf}$ at two temperatures appear in Table 2. At 20 °C intermolecular exchange of the CF_3CO_2^- group is rapid, indicated by quartet signals due to carbonyl carbons at $\delta 157.4$ with $^2J(^{13}\text{C}-\text{F}) = 37 \text{ Hz}$ and CF_3 carbons at $\delta 115.2$ with $^1J(^{13}\text{C}-\text{F}) = 290 \text{ Hz}$ for $[\text{Tl}(\text{tmpp})(\text{O}_2\text{CCF}_3)]$ in CD_2Cl_2 , but no $\text{Tl}-^{13}\text{C}$ splitting was observed. Likewise, at 20 °C, intramolecular exchange of the CF_3CO_2^- group is rapid, indicated by quartet signals due to both carbonyl carbons [$\delta 157.5$, $^2J(^{13}\text{C}-\text{F}) = 38 \text{ Hz}$] and CF_3 carbons [$\delta 115.0$, $^1J(^{13}\text{C}-\text{F}) = 290 \text{ Hz}$] for $[\text{Tl}(\text{tpp})(\text{O}_2\text{CCF}_3)]$ in CDCl_3 shown in Fig. 6(a), but still no $\text{Tl}-^{13}\text{C}$ splitting was

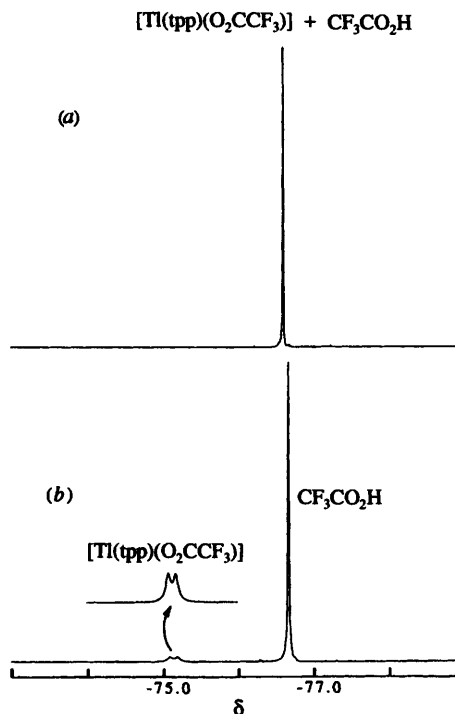


Fig. 5 The 282.40 MHz ^{19}F NMR spectra for $[\text{Tl}(\text{tpp})(\text{O}_2\text{CCF}_3)] + \approx 0.05 \text{ cm}^3 \text{ CF}_3\text{CO}_2\text{H}$ in $[\text{}^2\text{H}_8]\text{thf}$ at (a) 20 and (b) –100 °C

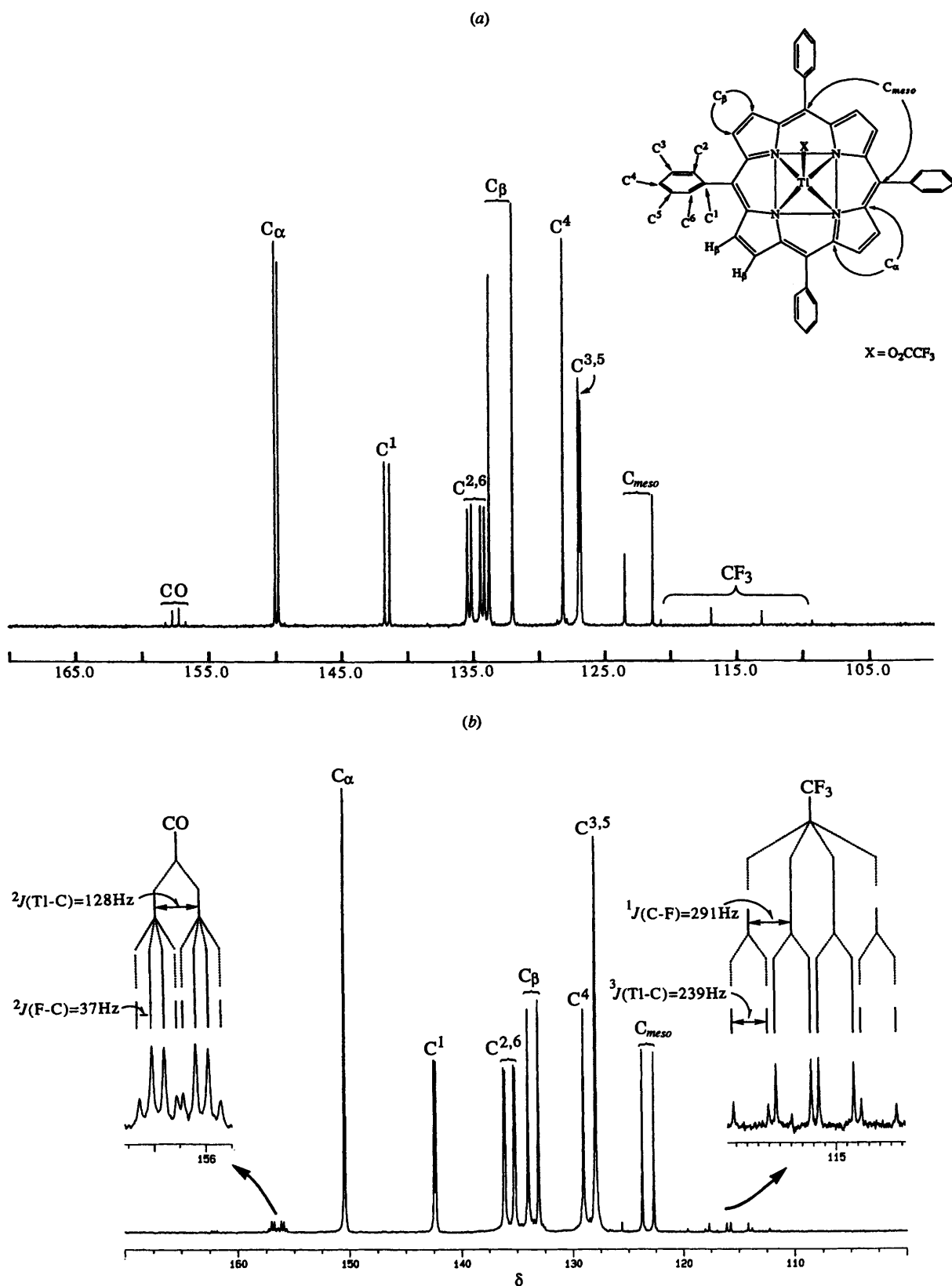


Fig. 6 The ^{13}C broad-band NMR spectra for $[\text{Tl}(\text{tpp})(\text{O}_2\text{CCF}_3)]$: (a) in CDCl_3 at 20°C (75.47 MHz), (b) in $[\text{}^2\text{H}_8]\text{thf}$ at -100°C (150.92 MHz)

observed. The $^1J(^{13}\text{C}-\text{F})$ and $^2J(^{13}\text{C}-\text{F})$ coupling constants of CF_3 and CO for $[\text{Tl}(\text{tpp})(\text{O}_2\text{CCF}_3)]$ and $[\text{Tl}(\text{tmpp})(\text{O}_2\text{CCF}_3)]$ at 20°C are quite similar to those of $[\text{TlR}(\text{O}_2\text{CCF}_3)_2]$ ($\text{R} = \text{aryl}$) whereas the resonances of CF_3 and CO for the former complexes are upfield compared with those of the latter complex [δ 118.5 ± 0.2 , $^1J(^{13}\text{C}-\text{F})$ 289.3 ± 2.3 Hz for CF_3 ; δ 161.2 ± 1.3 , $^2J(^{13}\text{C}-\text{F})$ $= 38.5 \pm 2.6$ Hz for CO].^{4,5}

At -100°C the rate of intramolecular exchange of CF_3CO_2^- for $[\text{Tl}(\text{tpp})(\text{O}_2\text{CCF}_3)]$ in $[\text{}^2\text{H}_8]\text{thf}$ is 1 Hz. This is slow comparable with the coupling frequency of $\text{Tl}-^{13}\text{C}$, *i.e.* 184 ± 56 Hz. Hence, the CO and CF_3 carbons of CF_3CO_2^- in $[\text{Tl}(\text{tpp})(\text{O}_2\text{CCF}_3)]$ shown in Fig. 6(b) are observed at δ 156.5 [$^2J(^{13}\text{C}-\text{F}) = 37$ and $^2J(\text{Tl}-^{13}\text{C}) = 128$ Hz] and 115.9 [$^1J(^{13}\text{C}-\text{F}) = 291$ and $^3J(\text{Tl}-^{13}\text{C}) = 239$ Hz], respectively.

Table 2 Carbon-13 NMR chemical shifts (δ) and thallium-carbon coupling constants (J in Hz) of $[\text{Tl}(\text{tmpp})(\text{O}_2\text{CCF}_3)]$ and $[\text{Tl}(\text{tpp})(\text{O}_2\text{CCF}_3)]$ in CD_2Cl_2 , CDCl_3 or $[\text{H}_8]\text{thf}^*$

Compound	$T/^\circ\text{C}$	C^4	C_α	$\text{C}^{2,6}$ ($\text{C}^{2,2'}$)		C^1	C_β	C_{meso}	$\text{C}^{3,5}$ ($\text{C}^{3,3'}$)		$p\text{-OCH}_3$	COCF_3	COCF_3
$[\text{Tl}(\text{tpp})(\text{O}_2\text{CCF}_3)]$ in CDCl_3 in $[\text{H}_8]\text{thf}$	20	128.1	149.9	135.2	134.2	141.5	132.8	122.4	126.9	—	—	115.0	157.5
	—100	129.1	150.5	136.1	135.2	142.4	133.6	123.2	128.0	—	—	115.9	156.5
$[\text{Tl}(\text{tmpp})(\text{O}_2\text{CCF}_3)]$ in CD_2Cl_2	20	160.1	150.4	136.5	135.7	134.0	132.9	122.4	112.7	55.8	—	115.2	157.4
	—90	158.5	149.0	135.8	135.3	132.6	132.3	121.5	111.6	55.0	—	115.2	157.4
				(20)	(23)	(29)	(135)	(161)	126.8			$^1J(\text{C-F}) = 290$	$^2J(\text{C-F}) = 38$
				(9)	(19)	(26)	(140)	(159)	127.9			$^1J(\text{C-F}) = 291$	$^2J(\text{C-F}) = 37$
				(17)	(21)	(28)	(139)	(160)	111.4			$^3J(\text{TI-C}) = 239$	$^2J(\text{TI-C}) = 128$
												$^1J(\text{C-F}) = 290$	$^2J(\text{C-F}) = 37$

* Chemical shifts in ppm relative to the centre line of CD_2Cl_2 at δ 53.6, to the centre line of CDCl_3 at δ 77.0 or to the centre line of the upfield resonance of $[\text{H}_8]\text{thf}$ at δ 25.3. Values in parentheses beneath are $J(\text{TI}-^{13}\text{C})$ coupling constants in Hz unless specified.

Table 3 Proton chemical shifts (δ) and thallium-proton coupling constants (J in Hz) for $[\text{Tl}(\text{tmpp})(\text{O}_2\text{CCF}_3)]$ and $[\text{Tl}(\text{tpp})(\text{O}_2\text{CCF}_3)]$ in CD_2Cl_2^a

Compound	$T/^\circ\text{C}$	H_β (β -pyrrole)	$\text{H}^{2,6}$ ($o\text{-H}$)		$\text{H}^{3,5}$ ($m\text{-H}$)		H^4 ($p\text{-H}$)	$p\text{-OCH}_3$
$[\text{Tl}(\text{tmpp})(\text{O}_2\text{CCF}_3)]$ in CD_2Cl_2	20	9.14 (72)	8.25 (7) ^b	8.05 (7)	7.34 (6) ^b	7.28 (7)	—	4.06
	—70	9.13 (76)	8.19 (7)	7.93 (8)	7.27 (7)	7.13 (8)	—	3.93
	r.t. ^c	9.10 (67)	8.15 (m)	—	7.27 (m)	—	—	4.18
$[\text{Tl}(\text{tpp})(\text{O}_2\text{CCF}_3)]$ in CD_2Cl_2	20	9.17 (73)	8.39 (s) ^d	8.20 (s)	7.82 (m) ^d	—	—	—
	—70	9.21 (76)	8.37 (5)	8.15 (7)	7.79 (m)	—	7.72 (6)	—
	r.t. ^c	9.09 (73)	8.26 (m)	—	7.82 (m)	—	—	—

^a Chemical shifts in ppm relative to CD_2Cl_2 at δ 5.3. Values in parentheses are $J(\text{TI-H})$ coupling constants in Hz. ^b $^3J(\text{H-H})/\text{Hz}$. ^c Room temperature; from ref. 2. ^d s = Singlet, m = multiplet.

Low solubility precluded observation of these ^{13}C resonances at -90°C for $[\text{Tl}(\text{tmpp})(\text{O}_2\text{CCF}_3)]$ in $[\text{H}_8]\text{thf}$ or CD_2Cl_2 .

The intermolecular (or intramolecular) exchange of the CF_3CO_2^- group is rapid for $[\text{Tl}(\text{tmpp})(\text{O}_2\text{CCF}_3)]$ {or $[\text{Tl}(\text{tpp})(\text{O}_2\text{CCF}_3)]$ } in CD_2Cl_2 (or CDCl_3) at 20°C , whereas rotation of the anisole (or phenyl) group along $\text{C}^1\text{-C}_{\text{meso}}$ bond is slow at the same temperature on the NMR time-scale for both compounds. This is supported either by the assignment of the peaks at δ 135.2, 134.2 (or 136.5, 135.7) to the $\text{C}^{2,6}$ carbons and 126.9, 126.8 (or 112.7, 112.5) due to the $\text{C}^{3,5}$ carbons (shown in Table 2) or by the assignment of the peaks of δ 8.25, 8.05 (or 8.39, 8.20) to the $\text{H}^{2,6}$ protons and 7.34, 7.28 (or 7.82) due to $\text{H}^{3,5}$ protons (in Table 3) for $[\text{Tl}(\text{tmpp})(\text{O}_2\text{CCF}_3)]$ {or $[\text{Tl}(\text{tpp})(\text{O}_2\text{CCF}_3)]$ }. Inequivalent o - and m -H protons at 20°C (Table 3) are observed for $[\text{Tl}(\text{tpp})(\text{O}_2\text{CCF}_3)]$ and $[\text{Tl}(\text{tmpp})(\text{O}_2\text{CCF}_3)]$ in this work while the literature data appear to show average values at room temperature.²

Conclusion

Trifluoroacetic acid results from the hydrolysis of $[\text{Tl}(\text{tmpp})(\text{O}_2\text{CCF}_3)]$ in CD_2Cl_2 , and both compounds, $\text{CF}_3\text{CO}_2\text{H}$ and $[\text{Tl}(\text{tmpp})(\text{O}_2\text{CCF}_3)]$, undergo intermolecular CF_3CO_2^- exchange. Neither complex $[\text{Tl}(\text{tpp})(\text{O}_2\text{CCF}_3)]$ nor $[\text{Tl}(\text{tmpp})(\text{O}_2\text{CCF}_3)]$ hydrolyse in $[\text{H}_8]\text{thf}$ and they undergo intramolecular CF_3CO_2^- exchange in this solvent. It is unclear why $[\text{Tl}(\text{tmpp})(\text{O}_2\text{CCF}_3)]$ hydrolyses to $\text{CF}_3\text{CO}_2\text{H}$ in CD_2Cl_2 but $[\text{Tl}(\text{tpp})(\text{O}_2\text{CCF}_3)]$ doesn't. Nevertheless this may be related to electron donation from the methoxy group in $[\text{Tl}(\text{tmpp})(\text{O}_2\text{CCF}_3)]$ to the TI^{3+} atom through the conjugated π system. This disperses the positive charge on TI, weakens the TI-O bond, and enhances the production of $\text{CF}_3\text{CO}_2\text{H}$ in CD_2Cl_2 solvent through equation (1). Furthermore, this is the first report of the observation of ^{13}C NMR data at low

temperature for the intramolecular CF_3CO_2^- exchange of $[\text{Tl}(\text{tpp})(\text{O}_2\text{CCF}_3)]$.

Acknowledgements

Financial support from the National Research Councils of the Republic of China under Grant NSC 85-2113-M-005-019 is gratefully acknowledged. J. H. Chen thanks Miss Peng-Chu Lan, Hui-Chi Tan and Nan-Leu Her (Hsin-Chu Major Instrument Centre) for help in measuring ^{13}C and ^{19}F NMR spectra, and Dr. Chu-Chieh Lin (National Chung-Hsing University) for help in measuring the single-crystal X-ray data.

References

- S. A. Moy, J. A. Gonzalez and L. J. Wilson, *Acta Crystallogr., Sect. C*, 1995, **51**, 1490.
- M. O. Senge, K. R. Senge, K. J. Regli and K. M. Smith, *J. Chem. Soc., Dalton Trans.*, 1993, 3519.
- L. Ernst, *Org. Magn. Reson.*, 1974, **6**, 540.
- L. Ernst, *J. Organomet. Chem.*, 1974, **82**, 319.
- W. Kitching, D. Praeger, C. J. Moore, D. Doddrell and W. Adcock, *J. Organomet. Chem.*, 1974, **70**, 339.
- W. Kitching, C. J. Moore, D. Doddrell and W. Adcock, *J. Organomet. Chem.*, 1975, **94**, 469.
- J. C. Chen, H. S. Jang, J. H. Chen and L. P. Hwang, *Polyhedron*, 1991, **10**, 2069.
- S. C. Suen, W. B. Lee, F. E. Hong, T. T. Jong, J. H. Chen and L. P. Hwang, *Polyhedron*, 1992, **11**, 3025.
- J. J. Fuh, S. S. Tang, Y. H. Lin, J. H. Chen, T. S. Liu, S. S. Wang and J. C. Lin, *Polyhedron*, 1994, **13**, 3031.
- G. M. Sheldrick, SHELXTL PLUS, Release 4.1, Siemens Analytical X-Ray Instruments, Madison, WI, 1991.
- D. M. Collins and J. L. Hoard, *J. Am. Chem. Soc.*, 1970, **92**, 3761.
- I. O. Sutherland, *Annu. Rep. N.M.R. Spectrosc.*, 1971, **4**, 71.

Received 23rd April 1996; Paper 6/02835G